BEHAVIOUR OF POST-TENSIONED TIMBER COLUMNS UNDER BI-DIRECTIONAL SEISMIC LOADING

Asif Iqbal[1], Stefano Pampanin[2], Alessandro Palermo[3] and Andrew H. Buchanan[4]

SUMMARY

Moment-resisting frames made of laminated veneer lumber (LVL) in combination with unbonded post-tensioning have recently been proposed for multi-storey timber buildings. Prefabricated and post-tensioned timber frames can be designed to have enhanced re-centering and energy dissipation after seismic loading. The unbonded post-tensioning provides re-centering capacity while energy is dissipated through the addition of special dissipating devices which also act as external reinforcing.

As part of a research program on multi-storey timber structures, this paper describes experimental and analytical studies to investigate the behaviour of post-tensioned LVL columns under uni-and bi-directional seismic loading. The results show excellent seismic performance, characterized by negligible damage of the structural members and small residual deformations, even under the combined effect of loading in two directions. Energy is dissipated mostly through yielding of external mild steel dissipaters connecting the column and the foundation, which can be easily removed and replaced after an earthquake. Since post-tensioning can be economically performed on site, the system can be easily implemented for either column-to-foundation connections in multi-storey timber buildings as well as for pier-to-foundation and/or pier-to-deck connections in timber bridges.

[1] *Structural Engineer, BRANZ Ltd., Wellington*

[2] *Professor, Department of Civil and Natural Resources Engineering, University of Canterbury, Christchurch*

[3] *Senior Lecturer, Department of Civil and Natural Resources Engineering, University of Canterbury, Christchurch*

[4] *Professor, Department of Civil and Natural Resources Engineering, University of Canterbury, Christchurch*

INTRODUCTION

Current seismic design philosophies for multi-storey buildings emphasize the importance of designing ductile structural systems which undergo many cycles of inelastic displacement during earthquakes, resulting in some residual damage but no significant reduction in strength. Innovative solutions have been developed under the U.S. PRESSS (PREcast Structural Seismic Systems) programme coordinated by the University of California, San Diego [1-3] for the seismic design of multi-storey precast concrete buildings. Such solutions are based on joints between pre-fabricated elements with unbonded post-tensioning. As a result, efficient structural systems are obtained, which can undergo large inelastic displacements, while limiting the damage to the structural system and assuring re-centring capability after the seismic event. A particularly efficient solution is provided by the "hybrid" system [4] where an appropriate combination of self-centring (unbonded tendons plus axial load) and energy dissipation (mild steel dissipating devices) produces a controlled rocking motion, characterized by a "flag-shaped" hysteresis loop (Figure 1). Similar solutions have been implemented in steel [5] showing that the PRESSS-technology can be successfully implemented regardless of the properties of the material used.

The hybrid concept has been recently proposed and implemented for engineered wood structures (Palermo *et al* 2005) and referred to as PRES-LAM system. In principle LVL (Laminated Veneer Lumber), Glulam (Glued laminated Timber), Cross-Lam, or X-Lam, (cross-laminated timber) could equally be adopted. In the experimental campaign herein reported focus was given to the use of Laminated Veneer Lumber. Fabricated from sheets of veneer glued into panels, LVL could be a well suited material for multi-storey timber construction, due to its higher level of homogeneity and superior strength when compared to rough sawn or, to a less extent, glue laminated timber. The randomization of wood defects and high quality control during manufacture leads to a nearly homogenous, yet highly orthotropic, material with low variability of mechanical properties.

As part of a comprehensive investigation on the development of innovative seismic systems for multi-storey timber construction, a number of different frame and wall systems have been successfully tested under uni-directional loading [5-9]. This paper investigates the use of these innovative self-centring ductile solutions for multi-storey timber buildings with seismic moment-resisting frames and jointed ductile connections.

Experimental results for hybrid exterior column-to-foundation subassemblies under cyclic quasi-static uni- and bi-directional loading are presented. Three unbonded post-tensioned solutions with different levels of initial post-tensioning and two hybrid solutions with external dissipaters are investigated for the column-to-foundation specimen under uni-directional loading. The results are critically discussed by highlighting the enhanced performance of the hybrid connections.

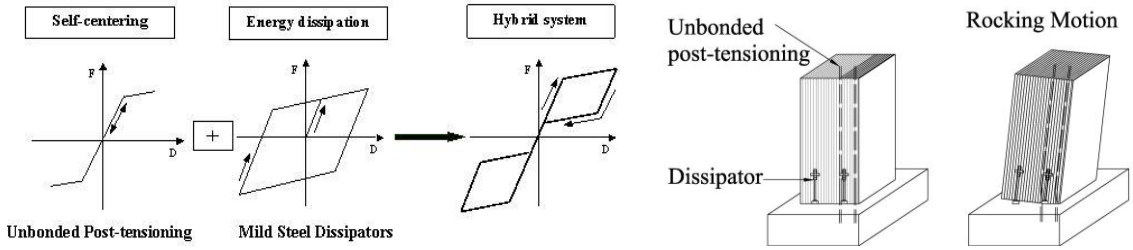


Figure 1: Flag-shaped hysteresis behaviour (left); Hybrid connection and rocking motion (right).

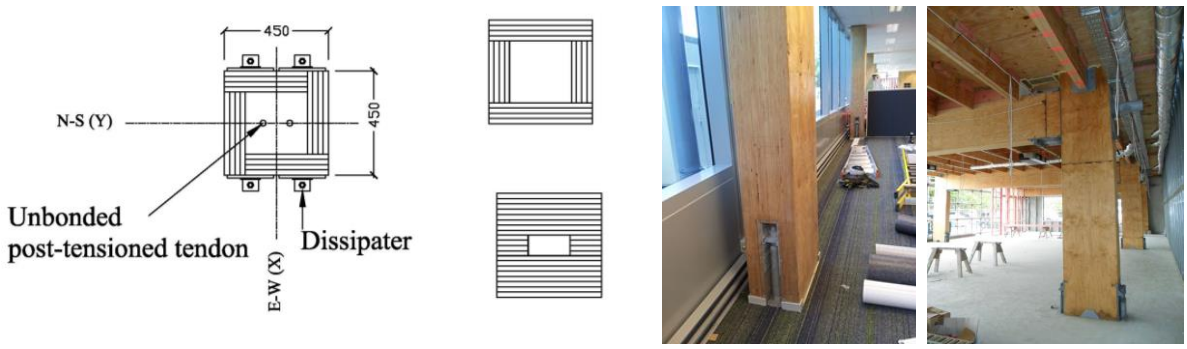


Figure 2: Column dimensions and component layout (left), Practical arrangements (right), (photos courtesy of BBR-Contech).

EXPERIMENTAL TESTS ON COLUMN TO FOUNDATION CONNECTIONS UNDER BI-DIRECTIONAL LOADING

In an actual multi-storey building frame, subject to ground shaking, the columns, especially the corner columns, are likely to undergo displacement demands in two directions simultaneously. Therefore, the focus of this experimental campaign was to test columns under a more realistic bi-directional load testing protocol (both quasi-static and pseudo-dynamic) and assess their performance against design assumption based on a more traditional uni-directional testing regime. A series of tests on cantilever timber columns connected to a steel foundation has been carried out. Both post-tensioned only solutions and hybrid solutions with external dissipaters were investigated. The experimental results for the column-to-foundation subassembly under bi-directional cyclic quasi-static and pseudo-dynamic loading are presented here. The results are discussed to evaluate the performance of the hybrid connections.

PROPERTIES OF THE SPECIMENS TESTED

The LVL used for the column is Hy90 [10], manufactured in accordance with AS/NZS 4357 by Carter Holt Harvey Woodproducts. For limit states' design to the New Zealand Standard, NZS 3603 [11], Hy90 characteristic strengths are given in Table 1.

Table 1. Material Properties of Hy90 [10]

Modulus of Elasticity Parallel to Grain	E	9000	MPa
Bending Strength	f'_b	35	MPa
Tension Strength Parallel to Grain	f'_t	19	MPa
Compression Strength Parallel to Grain	f'_c	28	MPa
Compression Strength Perp. to Grain	f'_p	10	MPa

The specimen was originally designed as a timber bridge pier to have the moment capacity close to that of a concrete bridge pier tested as part of a recent research project at University of Canterbury. However, the same elements can also be used as columns in a multi-storey timber building. The column was constructed to have a hollow section by gluing together four Hy90 standard beam sections, each with a width of 360 mm and thickness of 90 mm (Figure 2) to make a column 450 mm square. The hollow timber column could be upgraded to higher axial load capacity for high-rise building structures by either making the cavity smaller or adding high strength concrete infill while maintaining the unbonded post-tensioning arrangement. For commercial production it will be preferable to use the arrangement shown in Figure 2 for a large cavity or small cavity, because both of these can be manufactured in a standard press. An example practical arrangement is also shown in Figure 2 (right). Similar arrangements can be made for beam-to-column connections with the post-tensioning tendons in the beam passing through a cavity in the column. Post-tensioning bars can be used as an alternative to strands for the post-tensioning system.

A square sized steel base (Figure 3a) was used for the column specimens. While it provided the necessary options of anchoring the energy dissipaters, this was also a convenient solution for the series of tests with different specimens.

Half-circle shear keys (Figure 4c) were placed along all four sides of the column to stop the column from sliding on the steel base. The dissipaters were attached to the steel base through steel blocks welded to the base. The blocks had threaded holes in the centre which allowed the dissipaters to be put in and taken out easily, keeping the column specimen in place. The top ends of the dissipaters were attached to the faces of the column with brackets and steel plates (Figure 4b), which were fixed to the column with coach screws.

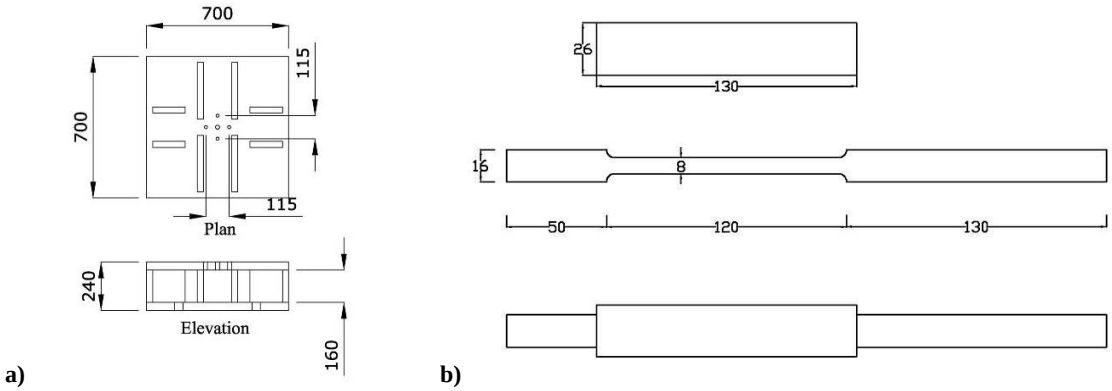


Figure 3: a) Steel base; b) Energy dissipaters used with the column.

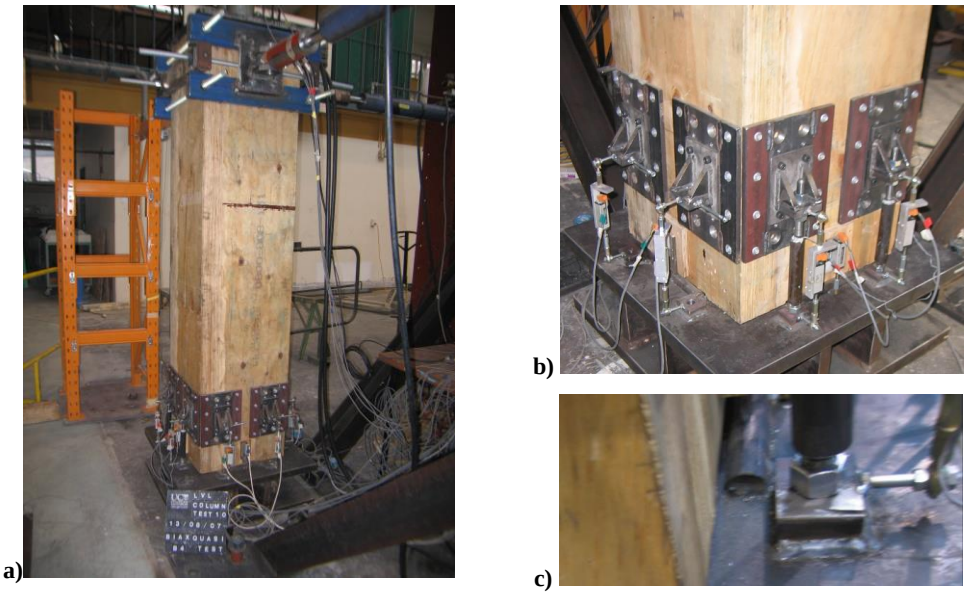


Figure 4: a) Testing arrangements; b) Column base; c) Shear keys at column side.

Table 2. Type and Properties of Specimens Tested

Specimen Type/ Designation	PT-only PT	Hybrid H1	Hybrid H2	Hybrid H3
Geometry (mm)	450 X 450	450 X 450	450 X 450	450 X 450
Initial Post-tensioning	145.0 kN (two tendons at 72.5 kN)	145.0 kN (two tendons at 72.5 kN)	87.0 kN (two tendons at 43.5 kN)	87.0 kN (two tendons at 43.5 kN)
Dissipation	None	4-8mm diameter at East & West faces	8-8mm diameter at all four faces	4-8mm diameter at North & South faces
Design λ	α	5.82	1.62	2.52

TEST SET-UP AND LOADING REGIME

A series of tests was carried out on a single column, subjected to bi-directional loading. There was no additional axial load applied and the initial post-tensioning in the two tendons was designed to include some axial force due to gravity load. A steel foundation was used for testing convenience although that is unlikely to represent practical applications. The bottom end of the timber column was placed directly on the steel foundation. No attempt was made to increase the bearing strength of the wood at the bottom end of the column nor to protect the corner edges from splitting failure. The post-tensioning tendons were anchored in a steel plate at the top of the column and under the steel foundation at the bottom. There was no other contact between the tendons and the column. The cantilever column was horizontally loaded at the expected point of contra-flexure within a frame system, i.e. the mid-level of the inter-storey height (Figure 5). The quasi-static loading protocol (Figure 6) consisted of cycles of increasing inter-storey drift, following the acceptance criteria for moment-frames proposed by the ACI T1.1-01 and ACI T1.1R-01 [12]. The load was applied simultaneously from two orthogonal directions through hydraulic actuators (Figure 5), which produced the resultant 'clover leaf' shaped protocol.

Mild steel fuse-type energy dissipaters (Figure 4b) were added to the column for the hybrid tests. The energy dissipaters consisted of steel rods designed to yield in both axial tension and in axial compression. In this case, the dissipaters consisted of a 300 mm long 16 mm diameter bars turned down to 8 mm for 120 mm of the length. The turned down parts were encased in steel tubes injected with epoxy to prevent buckling in compression. The top end of each external dissipater was connected to an external steel case fixed to the LVL column,

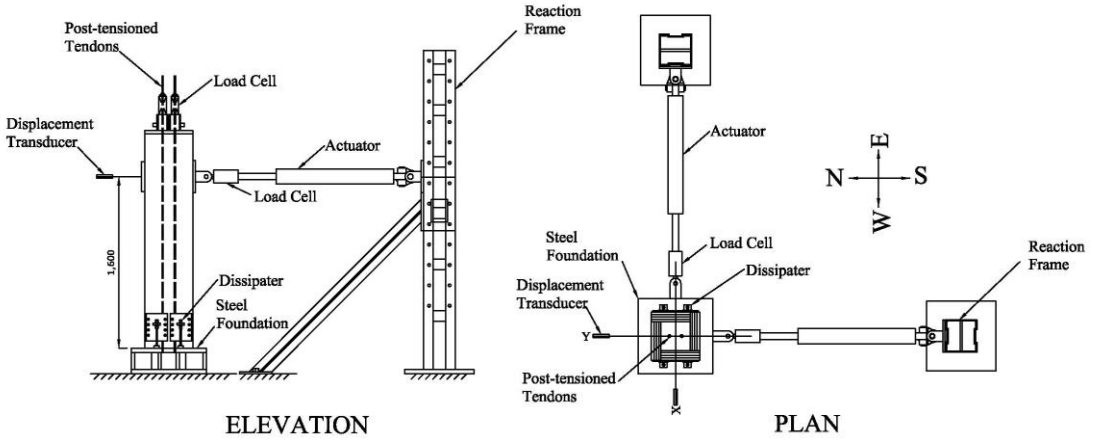


Figure 5: Test setup.

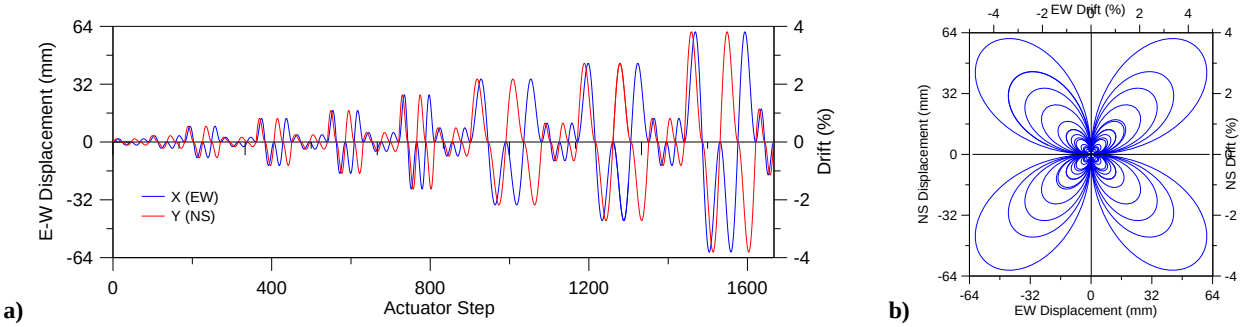


Figure 6: Loading protocol a) X and Y direction displacement demands; b) Combination.

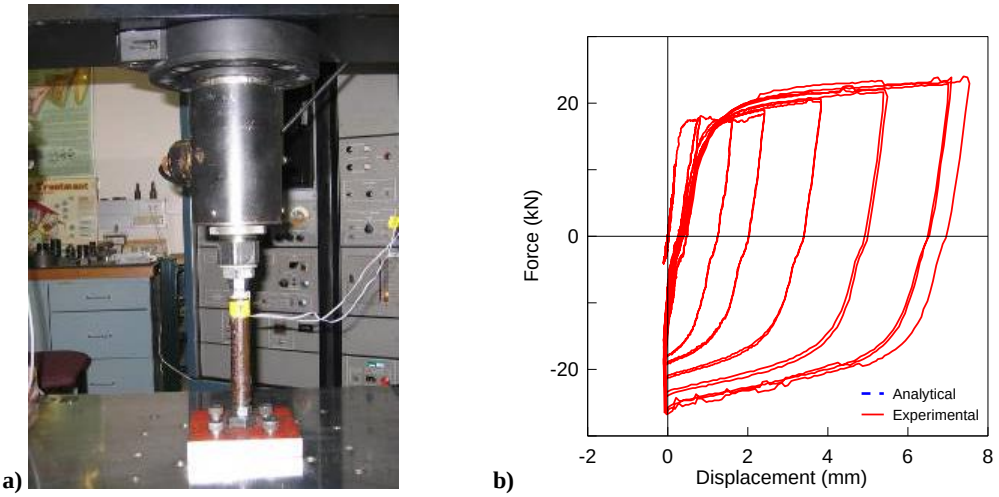


Figure 7: a) Steel base; b) Energy dissipaters used with the column.

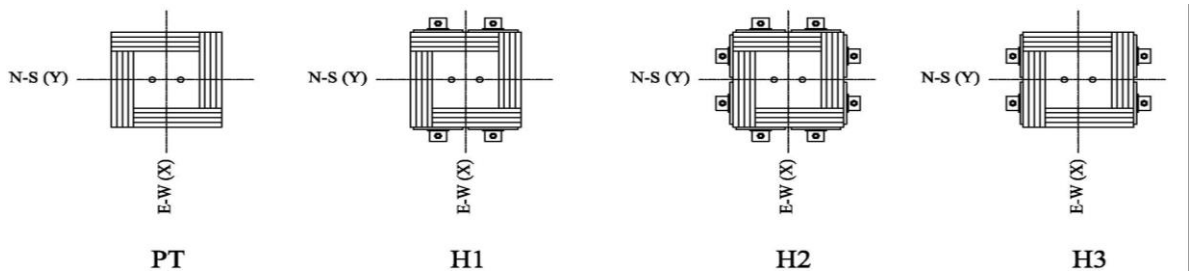


Figure 8: Details of specimens with designations.

and the bottom end was fixed to the steel foundation. Further details of the tests are presented in Iqbal [13-15].

QUASI-STATIC TESTS

Tests were carried out on the energy dissipating elements in order to confirm and characterize their behaviour. The axial dissipaters were tested under repeated cyclic loading simulating the deformations they were expected to go through during the tests of the column specimens. Quasi-static cyclic tests (Figure 7a) with increasing level of displacement (symmetric loading protocol) were carried out. These showed hysteresis loop with significant energy dissipation as shown in Figure 7b. The dissipater showed a post-yield stiffness of around 10% of initial stiffness.

In the quasi-static tests, the column was tested with post-tensioning only and with different arrangements of dissipaters to compare the recentering and dissipation characteristics of the different combinations as reported in Table 2. Figure 8 shows the details of the arrangements.

The column specimens were designed to re-centre fully after an earthquake. The re-centering ratio, as defined in NZS3101 - Appendix B (SNZ 2006) is:

$$\lambda = \frac{M_{PT} + M_N}{M_S} \geq 1.15$$

where, M_{PT} is the moment due to the post-tensioning, M_N is the moment due to gravity load on the column and M_S is the moment resistance provided by the energy dissipaters.

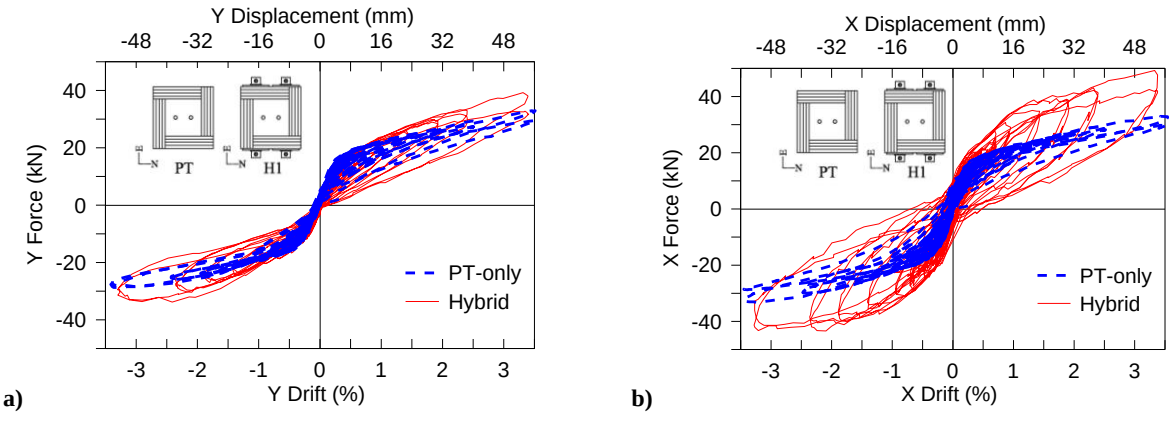


Figure 9: Load-displacement plots of specimens PT and H1 a) N-S direction; b) E-W direction.

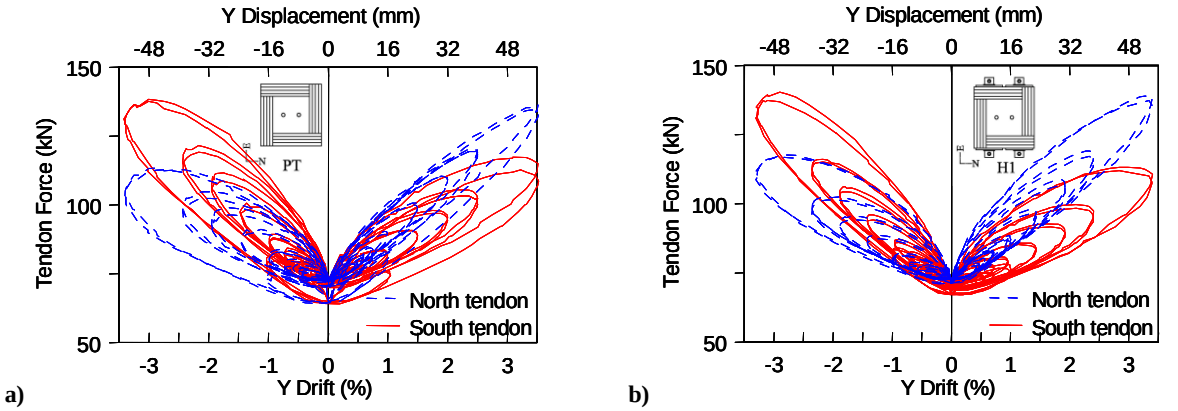


Figure 10: Plots of tendon forces vs. drift a) Specimen PT; b) Specimen H1.

After the bi-directional tests had been completed, it was decided to test the column under uni-directional loading to calculate the anticipated reduction in stiffness due to bi-directional loadings.

Specimen PT was tested with unbonded post-tensioning and no energy dissipaters. The blue lines on Figure 9(a) and Figure 9(b) illustrate the recorded values of lateral force vs. drift in the N-S and E-W directions respectively.

The tendon force vs. drift is shown in Figure 10(a). It is notable that there is some energy dissipation due to timber softening at the base of the column. Despite this inelastic deformation, the column base section did not suffer extensive damage during the test sequence.

The hybrid specimen H1 represents the preferred combination of post-tensioning and energy dissipation and has been used in previous column-to-foundation subassembly testing under uni-directional loading [6, 8]. It consists of two external dissipaters placed at each of the two sides parallel to the plane of the tendons. This configuration was also followed in this research, adding the dissipaters to the same column tested with post-tensioning only (Specimen PT). The red lines in Figure 9 illustrate the lateral force vs. drift. The tendon force vs. drift is shown in Figure 10(b). The neutral axis plots (Figure 11a) also show different locations of the neutral axis for the two directions, approximately equal to 0.6 and 0.3 of the column width, B, at 3.5% drift, respectively. The energy dissipation is calculated in terms of equivalent viscous damping ratio:

$$\xi = A_{tot}/4\pi A_{el}$$

Where A_{tot} is the energy dissipation per cycle and A_{el} is the elastic strain energy of the system. It is clear from Figure 12 that significant additional hysteretic dissipation with a maximum area-based equivalent viscous damping ξ of about 10% calculated from the force-drift values in the N-S direction and about 15% in the E-W direction is observed due to the presence of the energy dissipaters in the hybrid specimens. It is also important to notice that greater dissipation is achieved in the plane perpendicular to the tendons (E-W), but there are some residual displacements after loading in this direction. On the other hand, better re-centering is achieved in the direction parallel to their plane (N-S). This is because the ratio between re-centering moment and dissipating moment is 2.52, which is lower for the E-W direction compared to that of 5.82 for the N-S direction.

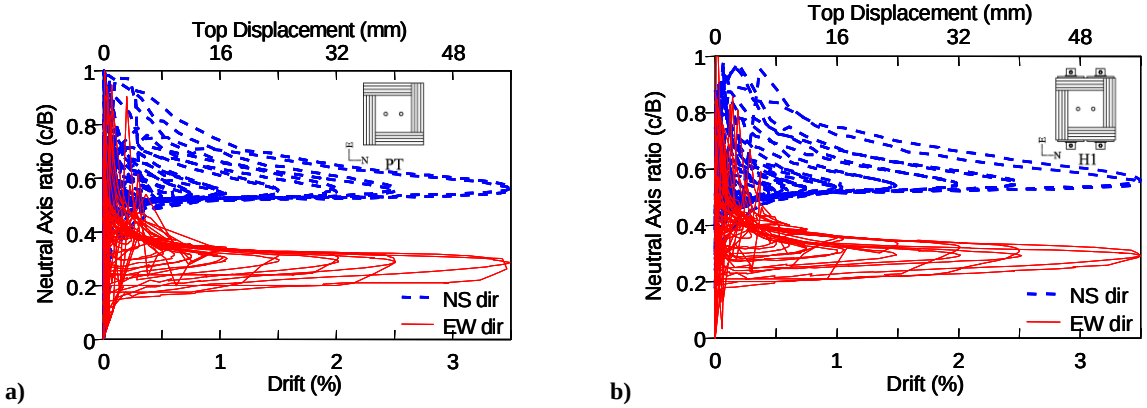


Figure 11: Plots of neutral axes locations: a) Specimen PT; b) Specimen H1.

PSEUDO-DYNAMIC TESTS

A series of pseudo-dynamic tests was carried out to simulate slow motion dynamic response of the system when subjected to an earthquake input ground motion, in both post-tensioned-only and hybrid configurations. The effects of different additional dissipation capacity on the dynamic response were investigated and provided valuable information complementary to that obtained from the quasi-static tests.

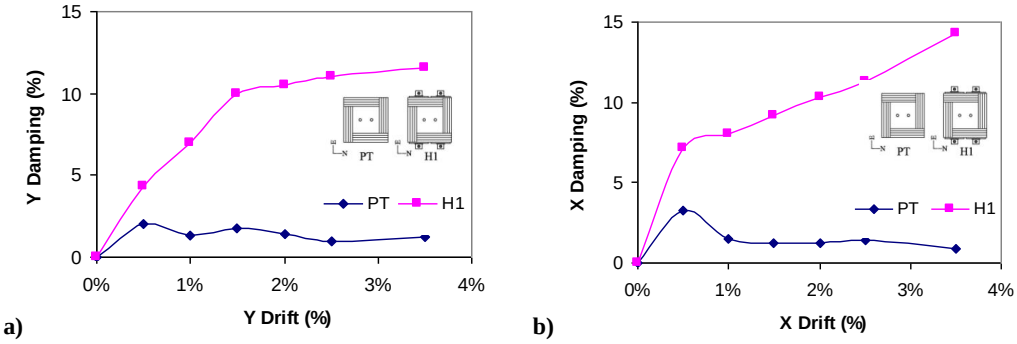


Figure 12: Damping-drift plots for PT and H1 in uni-directional tests a) N-S direction; b) E-W direction.

Table 3. Characteristics of the Adopted Earthquake Events (Dur is duration of shaking, Comp is the component direction)

Event	Year	Mw	Station	Dist (km)	Soil Type	Dur (sec)	Comp	PGA, g (scaled)
Landers	1992	7.3	Yermo Fire Station	24.9	D	44.0	360	0.334
							270	0.245
Cape Mendocino	1992	7.1	Fortuna Blvd	23.6	C	44.0	000	0.441
							090	0.433

The details of the earthquake ground motions used in the tests are given in Table 3. Figure 13 shows their response spectra compared to the New Zealand Loading Standard (NZ1170.5) acceleration design spectrum with a PGA of about 0.4g for soil class D and return periods of 500 and 2,500 years for a high seismicity area. For the hybrid column with dissipaters, the ground motions were scaled up to 150% which represent a return period of approximately 1,500 years according to New Zealand Standard NZS 1170.5 (SNZ, 2004).

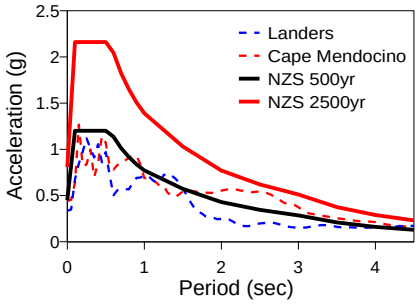


Figure 13: Response spectra of ground motions and standards.

Specimen PT was subjected to 100% of the earthquake record

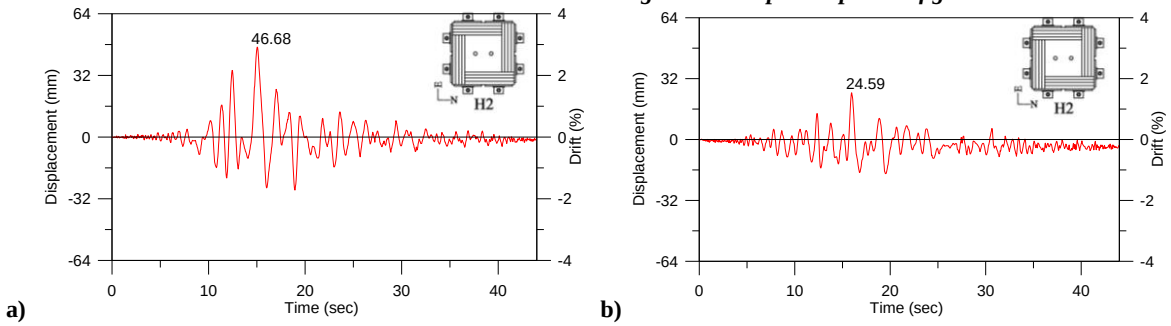


Figure 14: Response of Specimen H2 to Landers accelerogram a) N-S direction; b) E-W direction.

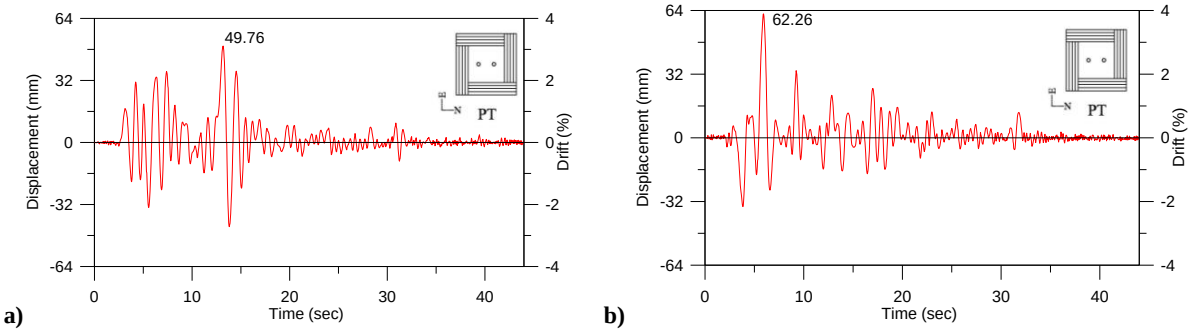


Figure 15: Response of Specimen PT to Cape Mendocino accelerogram a) N-S direction; b) E-W direction.

in both X and Y directions, which is very conservative since the combination will result in demands higher than that from a design level earthquake.

As part of the required information to solve the equation of motion of the SDOF system within the pseudo-dynamic algorithm, an equivalent mass of 4,500 kg was assumed. This corresponded to the expected gravity load (dead load plus 30% of the live load) for a 5 kPa load over a tributary area of 9 sq.m to a column within a single storey timber building. An equivalent viscous damping of 5% proportional to the initial stiffness was adopted.

The test of the post-tensioned only column could not be continued for the whole duration of the Landers accelerogram because the maximum drift exceeded the displacement limit of the actuators within the testing arrangement. The test on the hybrid specimen H1 could not be completed for the same reason. The hybrid specimen H2, having additional strength and dissipation capacity provided by the dissipaters, was subjected to a 50% higher intensity of the same earthquake record in order to investigate inelastic response and re-centring capability. In spite of the higher intensity of the ground motion, the maximum drift was less than the post-tension only case, due to the additional strength and dissipation contribution provided by the external dissipaters. The response of the hybrid solution subject to Landers accelerogram is shown in Figure 14. A small residual displacement is observed in the E-W direction due to the smaller out-of-plane re-centering capacity of the two prestressing tendons.

The column was tested post-tensioned only under recorded Cape Mendocino accelerogram scaled to have intensity comparable to the Landers earthquake (Table 3). Figure 15 shows the response of the post-tensioned only solution in terms of drift time-history. As expected, the maximum drift in this case is greater than that with the hybrid solution, but full re-centering is achieved despite partial asymmetry of the response.

FURTHER TESTING OF LVL COLUMN

It was observed after the first series of tests that there was some deterioration of properties of the column. The quasi-static loading protocol, consisting of three full clover-leaf cycles at each drift level, was deemed to be too demanding since a typical structure would not be expected to go through so many cycles of loading at such drifts. Another series of tests with fewer cycles of loading was therefore performed on a new column with identical properties to determine the degree of degradation of the column properties during the tests. Uni-directional benchmark tests were undertaken before and after the bi-directional quasi-static tests. The revised biaxial loading protocol included one full cloverleaf cycle at each drift in place of three cycles used in previous tests. The initial prestress level was also raised to 50% of yield stress to increase the re-centering capacity of the column and thereby eliminate the possibility of residual displacements observed in some of the earlier tests.

Figure 16 and Figure 17 show the comparative load-displacement plots before and after the post-tension only and hybrid biaxial test, respectively. No significant degradation of strength was observed during the biaxial testing of the column. This means that no additional protection is required at the connections in practical applications since the structure is unlikely to experience more than one or two major earthquakes during its lifetime.

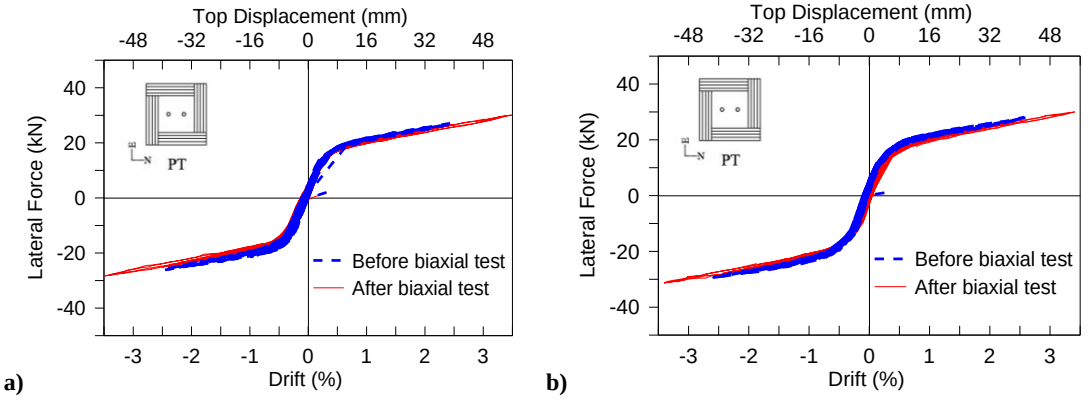


Figure 16: Plots of Specimen PT before and after biaxial test a) N-S direction; b) E-W direction.

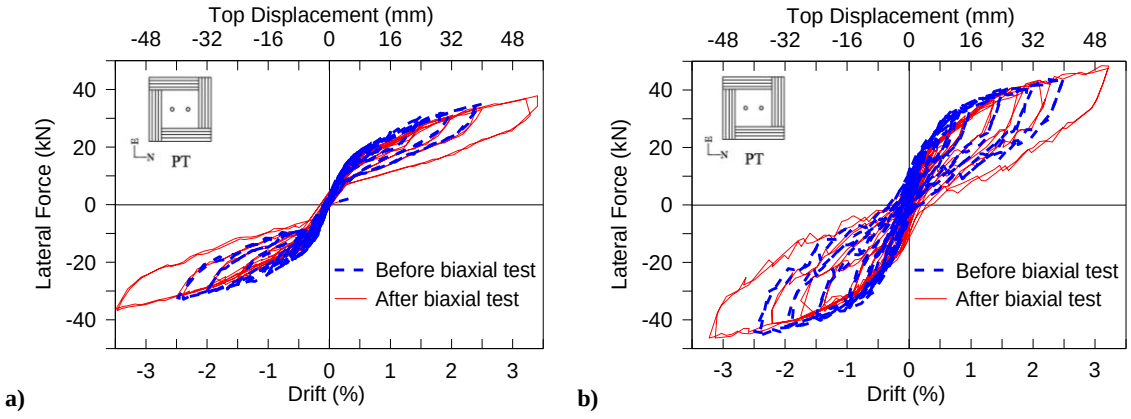


Figure 17: Plots of Specimen H1 before and after biaxial test a) N-S direction; b) E-W direction.

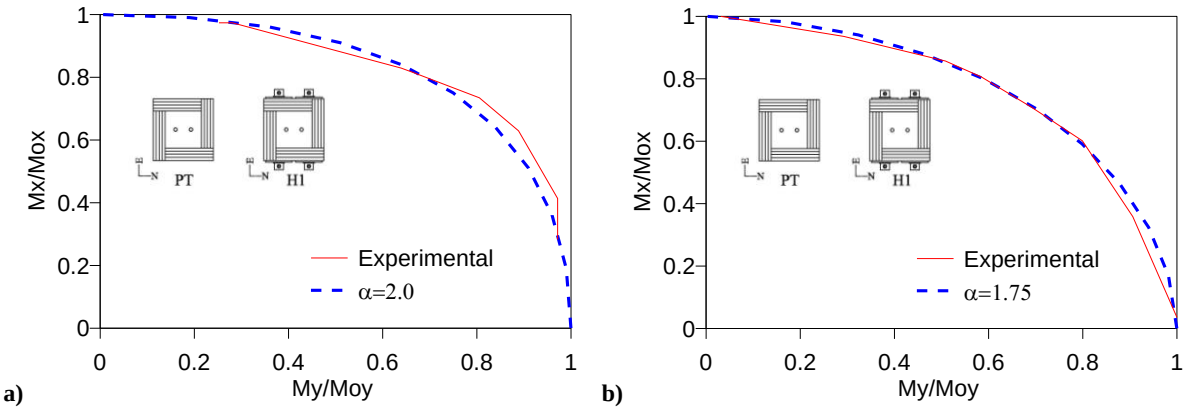


Figure 18: Interaction Plots of Specimen H1 a) Specimen PT; b) Specimen H1.

BI-DIRECTIONAL LOADING EFFECTS

The general failure surface of a symmetric column section under biaxial bending is expressed by an elliptical formulation proposed by Bresler [16]. The effects of bi-directional response can be plotted within an M_x-M_y diagram:

$$(M_x/M_{ox})^{\alpha} + (M_y/M_{oy})^{\alpha} = 1$$

Where

M_x = x-axis component of the biaxial applied moment

M_y = y-axis component of the biaxial applied moment

M_{ox} = capacity of the section about the principle x-axis

M_{oy} = capacity of the section about the principle y-axis

α is the exponent indicating the degree on interaction. For no interaction between the two directions the value of α would be zero, whereas α value of 1.0 means linear interaction.

The applied moment values are taken from the experimental results while the maximum moments at 3.5% drifts, which are close to ULS, are taken as the capacity. As explained by Marriott *et al;* [17, 18], the 3-dimensional lateral response of a column section is dependant on the displacement path. A biaxial plot matching the displacement path followed by the clover-leaf shaped experimental protocol is indicative of the level of interaction.

The effects of interaction between moment capacities in two orthogonal directions during bi-directional loading at 3.5% drift are plotted in Figure 18. The values of α that better fit the experimental results, namely 2.0 and 1.75 for the PT and H1 specimens, respectively, indicate that the moment capacity in one direction is affected by simultaneous loading in the other direction. This phenomenon, also shown for bi-directional testing of unbonded post-tensioned and dissipative precast concrete column/piers (Marriott *et al.*, 2011), should be accounted for in the design process.

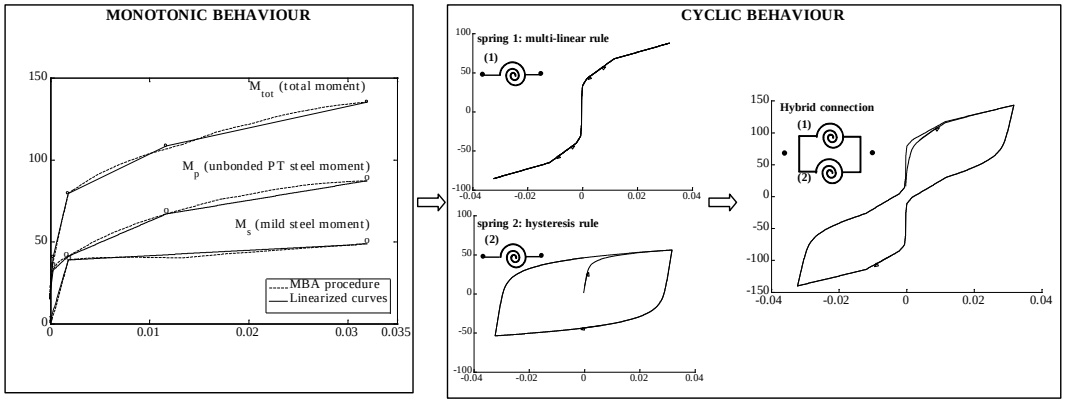


Figure 19: Calibration of springs referring to Monotonic Beam Analogy [22}.

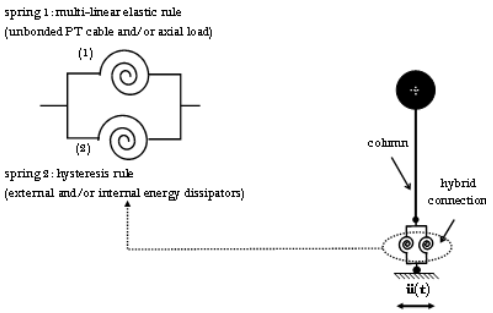


Figure 20: Lumped Plasticity model of Column [22}.

ANALYTICAL STUDY

In order to facilitate the practical day-to-day design of these innovative structures, it is necessary to develop simplified analytical models of these solutions for practical structures. A preliminary numerical model of one column-to-foundation system is described below. A simple analytical approach based on a section analysis concept and lumped plasticity model [18] is followed to calculate the bi-directional behaviour of the column. Although the procedure was originally developed for precast concrete structures [19-20], it has been found applicable to timber structures with minor adjustments [21].

As proposed in previous literature on jointed ductile connections (Pampanin *et al.*, 2001, [19]) a lumped plasticity model can be efficiently adopted for hybrid connections where the main inelastic demand is accommodated within discrete critical sections (i.e. at the column-foundation interface). Due to the opening and closing of a single crack at the interface, an infinite curvature is developed at the critical section: therefore a moment-rotation relationship has to be preferred to a traditional moment-curvature when characterizing the section behaviour. Rotational inelastic springs in parallel, with appropriate hysteretic behaviour, are assigned to represent the inelastic action at the column-foundation interface while elastic elements are used to represent the structural members.

Figure 20 shows the Lumped Plasticity model of the column, as implemented with the Ruaumoko [24] finite-element code. A three-dimensional model of the column and its base connection was created to apply the bi-directional loading. A bi-linear elastic (or non-linear elastic, NLE) hysteresis rule was used to model the post-tensioning tendons while a modified Takeda [25] hysteresis rule was used to model the contribution of the energy dissipaters. Figure 21 and Figure 22 show the comparison between the analytical and experimental results for the post-tensioned only, PT, and the hybrid solution, H1, respectively. In general, satisfactory confirmation of the reliability of the analytical/numerical procedure was established from the plots.

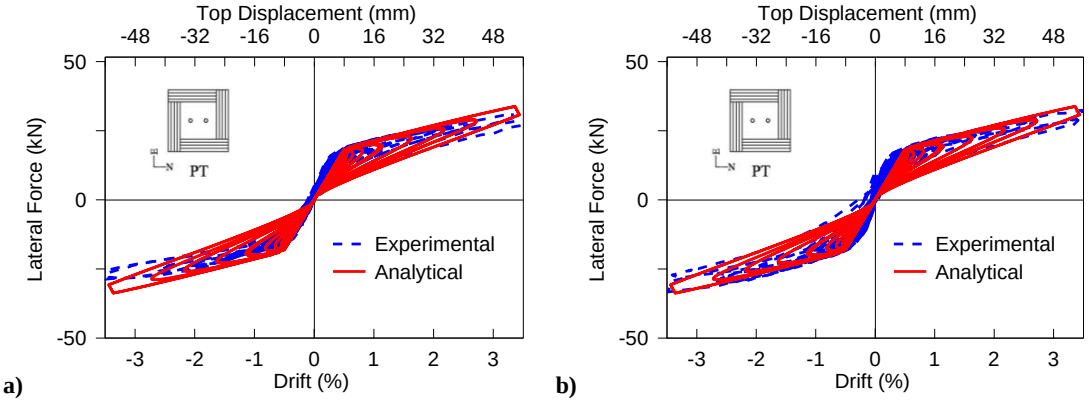


Figure 21: Comparative plots of lumped plasticity model of PT-only specimen: a) N-S direction; b) E-W direction.

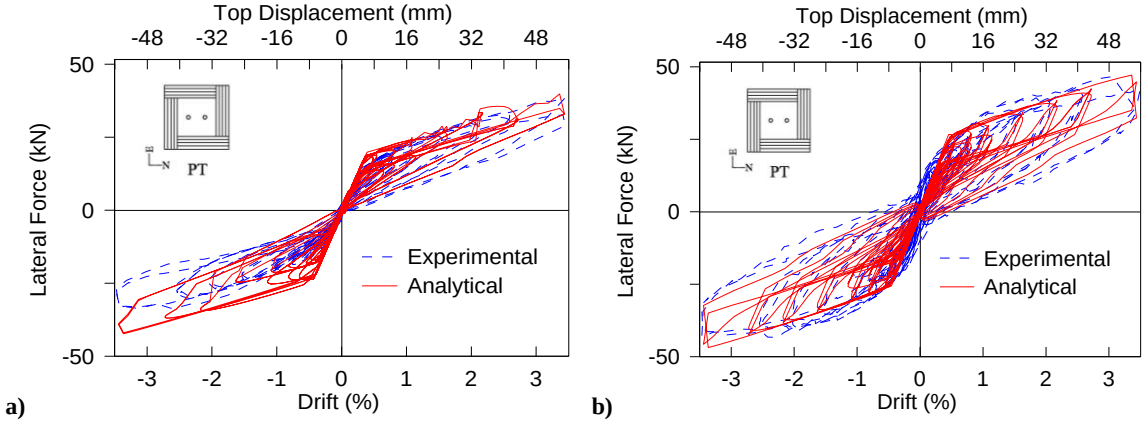


Figure 22: Comparative plots of lumped plasticity model of Hybrid specimen: a) N-S direction; b) E-W direction.

One rotational spring is assigned a nonlinear elastic rule to represent the self-centring contribution, while for the second spring a hysteresis rule representing the energy dissipation contribution is adopted.

The calibration of the two rotational springs can be obtained by evaluating the monotonic moment-rotation behaviour of each contribution, i.e. mild steel energy dissipation devices and post-tensioning tendons, referring to the Monolithic Beam Analogy (MBA) procedure originally proposed by Pampanin *et al.* [19] and subsequently refined by Palermo [20], which relies on member compatibility in terms of displacements between a monolithic and a hybrid solution. As represented in Figure 19, each curve contribution obtained adopting the MBA can be linearized referring to the fundamental performance levels, i.e. the decompression point, loss of linearity point, yielding, serviceability and failure point. Figure 19 summarizes the above mentioned calibration procedure assuming a Ramberg-Osgood [23] hysteresis rule for the cyclic behaviour of the dissipater.

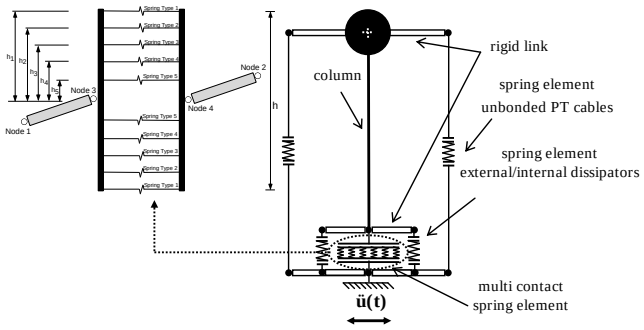


Figure 23: Multi-Spring model of Column [22].

The column behaviour was also modelled using an alternative approach called the Multi-Spring model which had the advantage in predicting the local behaviour, i.e. neutral axis position, stresses. In place of rotational springs in parallel, the Multi-Spring approach uses a series of axial springs in parallel

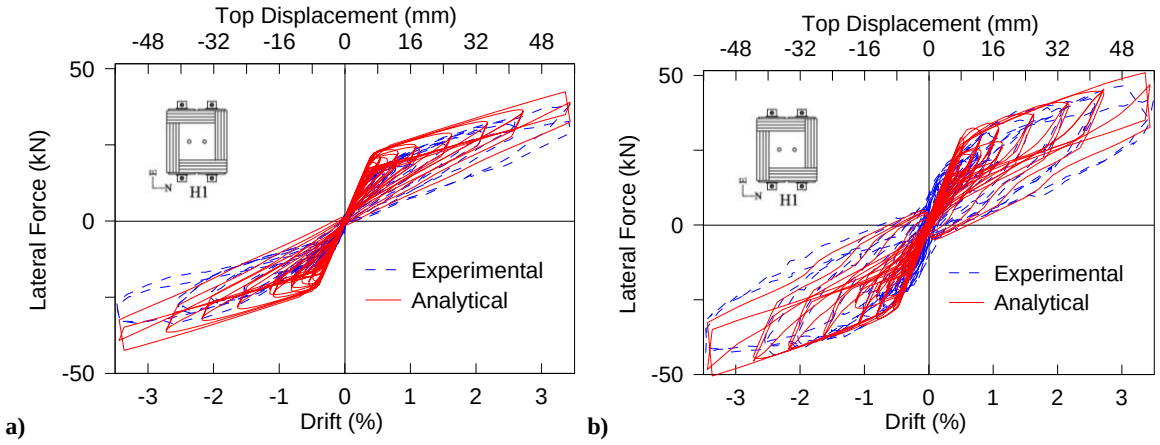


Figure 24: Multi-spring model plots of Hybrid specimen: a) N-S direction; b) E-W direction.

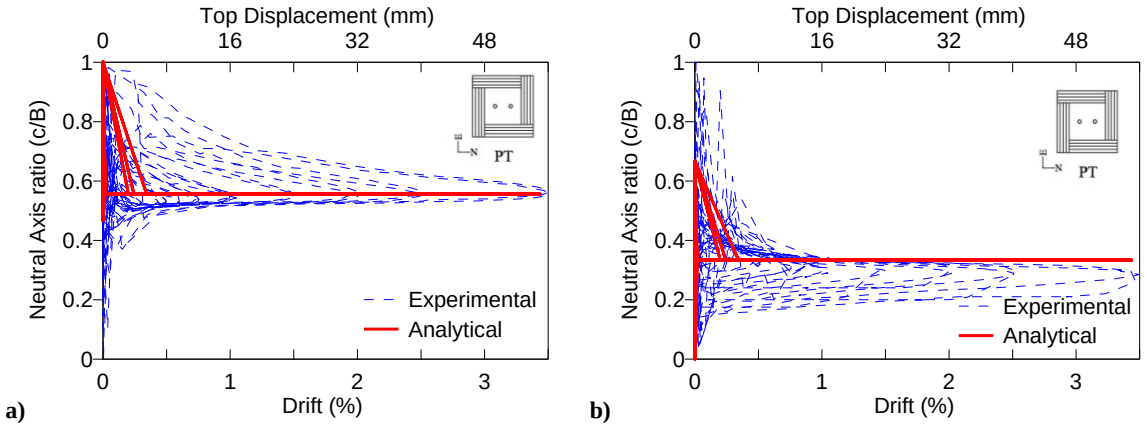


Figure 25: Neutral axis locations of PT-only specimen: a) N-S direction; b) E-W direction.

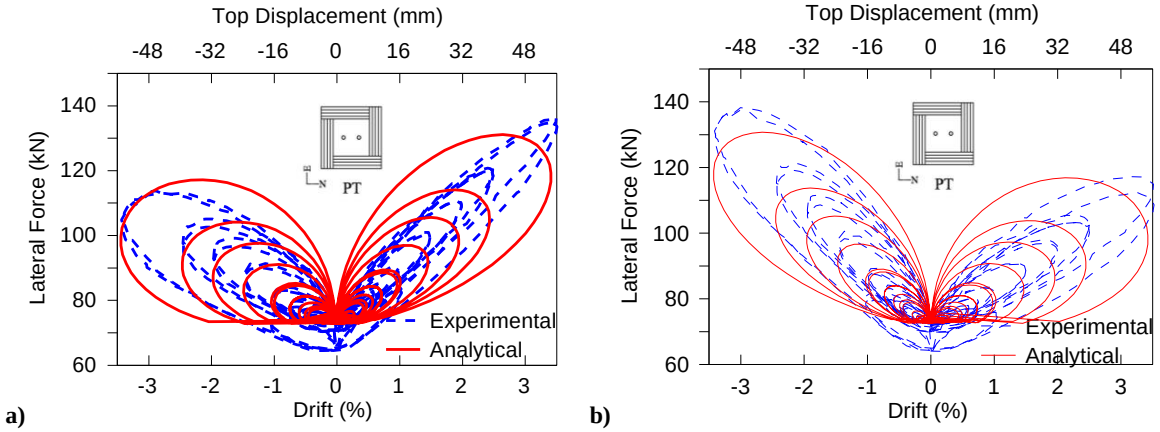


Figure 26: Tendon forces of PT-only specimen: a) North tendon; b) South tendon.

to model the rocking behaviour at the contact section interface. Unlike the lumped plasticity model, the multi-spring model can incorporate axial deformations of the member and can also predict the location of the neutral axis.

The column-to-foundation connection modelled using the multi-axial spring concept is shown in Figure 23. The three-dimensional model was implemented with Ruaumoko [24].

A compact multi-spring fine-element was used to represent the contact interface, while the contribution of the tendons was modelled using a dedicated axial spring element anchored at the top and bottom of the column, to properly represent the unbounded length. Similarly a dedicated axial spring/element with a Dodd-Restrepo [26] hysteretic rule was adopted to represent the energy dissipaters. The model of the dissipater was calibrated against the separate dissipater test result.

The load-deflection plot of the hybrid column, H1 is compared with the results of the model in Figure 24. Although the loops in the negative drift region are not typically shaped due to the characteristics of the hysteresis model used, the model is in good agreement with the experimental results in general.

The comparisons of the neutral axis plots for the PT-only specimen are shown in Figure 25. Results from the model are within a relatively narrow band compared to the gradual convergence in the test results, but the base lines match reasonably well in the two results. The tendon forces vs. drift comparisons in Figure 26 showed reasonable agreement in terms of the limits, although the shapes of the loops are slightly different.

CONCLUSIONS

The results of cyclic quasi-static and pseudo-dynamic experiments on column-to-foundation connections under bi-

directional loading confirm the viability of hollow post-tensioned LVL columns in multi-storey timber frame buildings with hybrid connections. As expected, the hybrid systems showed a significantly greater level of energy dissipation than the post-tensioned only systems, which allows for lower displacement demand when subjected to pseudo-dynamic loading. In all cases, considering different simulations of seismic loading, the tested systems exhibited high levels of ductility, negligible residual deformations and no significant damage. Analytical studies show good agreement between the experimental and numerical results indicating that the behaviour of the system in practical applications can be predicted with a high level of confidence.

The section analysis procedure for design is illustrated through a worked example in the Appendix.

ACKNOWLEDGMENTS

The research for this paper received financial support from Forest Industries Development Agenda (FIDA) and Structural Timber Innovation Company (STIC), respectively for the experimental part and the subsequent numerical investigations. The LVL used in the specimens was supplied by Carter Holt Harvey New Zealand. Massimo Fragiacomo of University of Sassari, Italy provided some suggestions for the experiments. The laboratory staff of the Department of Civil and Natural Resources Engineering, University of Canterbury helped in preparation of the specimens and also with the experimental setup. The support of these organizations and people is gratefully acknowledged.

APPENDIX

Section Analysis of Column with Hybrid Test Specimen: Worked Example

Steps to determine connection flexural capacity:

Connection rotation, θ_{imp} is imposed

Drift, $\theta = 2\%$

Neutral axis depth (through trial),

$c = 0.18D = 80.8$ mm

Elongation of the tendon, Δ_{pt1} =4.03 mm and Δ_{pt2} = 1.03 mm.

To check the tendon is not yielding,

$\varepsilon_{pt1} = 0.00212$ and $\varepsilon_{pt2} = 0.00091$

$\varepsilon_{pti} = 0.0039$, $\varepsilon_{ps} = 0.0078$, $0.9\varepsilon_{ps} = 0.007$

$\varepsilon_{pti} + \varepsilon_{pt1} = 0.006 < 0.9\varepsilon_{ps}$

$\varepsilon_{pti} + \varepsilon_{pt2} = 0.0048 < 0.9\varepsilon_{ps}$

Elongation in energy dissipaters,

Tension steel: $\Delta stt = 5.56$ mm

Compression steel: $\Delta stc = -0.56$ mm

Strain in the dissipater,

$\varepsilon_{st} = 0.0556$

$\varepsilon_{sc} = 0.0056$

To make sure the dissipater has yielded,

Yield strain of steel, $\varepsilon_{yst} = 0.0015 < \varepsilon_{st}, \varepsilon_{sc}$

Strain in the timber from Monolithic Beam Analogy: $\varepsilon_t = 0.00306$

Where, L_{cant} the shear span = 0.5*3200 = 1,600 mm

And the decompression curvature, φ_{dec} = 3.4E-7,

To check the timber is not yielding,

$\varepsilon_{y,t} = 28/(.55*9000) = 005657 > \varepsilon_t = 0.00306$

The compressive force in the timber is calculated: $C_t = 275.1$

$\Delta T_1 = 42$ kN and $\Delta T_2 = 18.1$ kN

$T_{initial} = 77$ kN, $T_{pt1} = 119.3$ kN and $T_{pt2} = 95.3$ kN.

$T_{pt} = 214.6$

Dissipater in tension: $T_s = 30.2$ kN

Dissipater in compression: $C_s = 30.2$ kN (tension)

Connection equilibrium condition: $T_{pt}+N+T_s+C_s = 274.9 \approx C_t$, Satisfied

Moment capacity, M_{pt} = 43.87 kN-m, M_s = 7.54 kN-m, φM_{pt} = 46.27 kN-m, λ= 5.82

REFERENCES

1 Priestley, M.J.N., 1991. Overview of the PRESSS Research Program, *PCI Journal*, Vol. **36**(4), pp.50-57.

2 Priestley, M.J.N., 1996. The PRESSS Program –Current Status and Proposed Plans for Phase III, *PCI Journal*, Vol. **41**(2), pp.22-40.

3 Priestley, M.J.N., Sritharan, S., Conley, J. R. and Pampanin, S., 1999. Preliminary Results and Conclusions from the PRESSS Five-story Precast Concrete Test-building, *PCI Journal*, **44**(6), 42-67.

4 Stanton, J.F., Stone, W.C. and Cheok, G.S., 1997. A Hybrid Reinforced Precast Frame for Seismic Regions, *PCI Journal*, **42**(2), 20-32.

5 Christopoulos, C., Filiatrault, A., Uang, C.M. & Folz, B. 2002. Post-tensioned Energy Dissipating Connections for Moment Resisting Steel Frames, ASCE Journal of Structural Engineering, Vol. **128**(9), 1111-1120.

5 Palermo, A., Pampanin, S., Buchanan, A. and Newcombe, M. 2005. Seismic Design of Multi-storey Buildings using Laminated Veneer Lumber (LVL), *Proc. NZSEE Conference*, Wairakei, New Zealand, CD-ROM.

6 Palermo, A., Pampanin, S., Fragiacomo, M., Buchanan, A.H. and Deam, B.L. 2006. Innovative Seismic Solutions for Multi-storey LVL Timber Buildings, *Proc. of 9th World Conference on Timber Engineering*, Portland, Oregon, CD-ROM.

7 Palermo, A., Pampanin, S., and Buchanan, A., 2006. Experimental Investigations on LVL Seismic Resistant Wall and Frame Subassemblies, *Proc. of First European Conference on Earthquake Engineering and Seismology*, Geneva, Switzerland, CD-ROM.

8 Palermo, A., Pampanin, S., Fragiacomo, M., Buchanan, A.H., Deam, B.L. and Pasticier, L., 2006.Quasi-static cyclic tests on seismic-resistant beam-to-column and column-to-foundation subassemblies using Laminated Veneer Lumber (LVL), *Proc. of Australasian Conference on Mechanics and Materials*, Christchurch, New Zealand.

9 Smith, T., Ludwig, F., Pampanin, S., Fragiacomo, M., Buchanan, A., Deam, B. and Palermo, A., 2007. Seismic Response of Hybrid-LVL Coupled Walls under Quasi-static and Pseudo-dynamic Testing, *Proc. NZSEE Conference*, Palmerston North, New Zealand, CD-ROM.

10 Futurebuild 2003. *Engineered Building Products: Information for Design and Installation*, Carter Holt Harvey Limited, Auckland, New Zealand.

11 SNZ. 1993. NZS 3603. *Timber Structures Standard*, Standards New Zealand, Wellington, New Zealand.

12 ACI T1.1-01 and ACI T1.1R-01 2001. *Acceptance Criteria for Moment Frames Based on Structural Testing (T1.1-01) and commentary (T1.1R-01)*, ACI Innovation Task group 1 and Collaborators.

13 Iqbal, A., Pampanin, S. and Buchanan, A.H., "Experimental Study of Prestressed Timber Columns under Bi-directional Seismic Loading", *Proc. NZSEE Conference*, Wairakei, 2008.

14 Iqbal, A., Pampanin, S. and Buchanan, A.H., "Seismic Behaviour of Prestressed Timber Columns under Bi-directional Loading", *Proc. 10th WCTE*, Miyazaki, 2008.

15 Iqbal, A., "Seismic Response and Design of Subassemblies for Multi-Storey Prestressed Timber Buildings", Ph D. thesis. University of Canterbury (submitted), 2010.

16 Bresler, B. "Design criteria for reinforced concrete columns under axial load and biaxial bending", *ACI Journal, 57*(11), 1960, pp 481-490.

17 Marriott, D.J. "The Development of High-Performance Post-Tensioned Rocking Systems for the Seismic Design of Structures", Ph D thesis, University of Canterbury, 2009.

18 Marriott, D., Pampanin, S., Palermo, A., 2011, 'Biaxial Testing of Unbonded Post-Tensioned Rocking Bridge Piers with External Replaceable Dissipaters, *Earthquake Engineering and Structural Dynamics*, **40** (15), 1723-1741

19 Palermo, A., Pampanin, S. and Carr, A.J. "Efficiency of simplified alternative modelling approaches to predict the seismic response of precast concrete hybrid systems", *Proc. fib Symposium* "Keep Concrete Attractive", Budapest, Hungary, 2005.

20 Pampanin, S., Priestley, M.J.N. and Sritharan, S., 'Analytical Modelling of the Seismic Behaviour of Precast Concrete Frames Designed with Ductile Connections', *Journal of Earthquake Engineering*, **5**(3), 2001, pp 329-367.

21 Palermo, A. "The Use of Controlled Rocking in the Seismic Design of Bridges", Ph D thesis, Technical University of Milan, Italy, 2004.

22 Newcombe, M.P., Pampanin, S., Buchanan, A.H. and Palermo, A. "Section Analysis and Cyclic Behavior of Post-Tensioned Jointed Ductile Connections for Multi-Story Timber Buildings", *Journal of Earthquake Engineering*, **11** (Special Edition), 2008, pp 83-110.

23 Ramberg, W. and Osgood, W.R., "Description of Stress-Strain Curves by Three Parameters", National Advisory Committee on Aeronautics, Technical Note 902, 1943.

24 Carr, A.J., "RUAUMOKO Program for Inelastic Dynamic Analysis – Users Manual", Department of Civil Engineering, University of Canterbury, New Zealand, 2005.

25 Otani, S., "Hysteresis Models of Reinforced Concrete for Earthquake Response Analysis", *J. Faculty of Engineering, University of Tokyo*, Tokyo, Vol. XXXVI, No. 2, 1981, pp 125-159.

26 Dodd, L.L. and Restrepo-Posada, J.I. "Model for Predicting Cyclic Behaviour of Reinforcing Steel", *J. Structural Engineering, ASCE*, **121**(3), 1995, pp 433-445.